Proceedings of Basic and Applied Sciences
ISSN 1857-8179 (paper). ISSN 1857-8187 (online). http://www.anglisticum.mk
Proceedings of the 1st International Conference on New Horizons in Basic and Applied Science, Hurghada – Egypt, Vol 1(1), 2013.

Structural and Optical Properties of Znse1−Xtex Nanocrystalline Thin Films in Terms of Optical Spectroscopic Ellipsometry

E.R. Shaaban[a], M. Emam-Ismail[b], M. El-Hagary[c], A.M. Abd Elnaeim[a] ,A. Adel[a]
[a]Physics Department, Faculty of Science, Al-Azhar University, 71452 Assuit, Egypt
[b]Physics Department, Faculty of Science, Ain Shams University, 11566 Cairo, Egypt
[c]Physics Department, Faculty of Science, Helwan University, Helwan, 11792 Cairo, Egypt
*E-mail of the Corresponding author: esam_ramadan2008@yahoo.com

Received November 13, 2013; Revised November 14, 2013; Accepted November 15, 2013

Abstract: *Polycrystalline thin films of $ZnSe_{1-x}Te_x$ ($0.0 \le x \le 1.0$) were deposited on glass substrate using electron beam deposition technique. The structure of the prepared films was examined using X-ray diffraction technique and revealed that the deposited films have polycrystalline zinc blend structure. The optical constants and film thicknesses of nanocrystalline $ZnSe_{1-x}Te_x$ films were obtained by fitting the spectroscopic ellipsometric data (ψ, Δ) using a three-layer model system in the wavelength range from 400 to 1100 nm. The refractive index was observed to increase with increasing Te concentration. This increase in the refractive index with increasing Te content may be attributed to the increase in the polarizability due to the large ionic radius of Te compared to the ionic radius of Zn. The optical studies of the polycrystalline $ZnSe_{1-x}Te_x$ films showed that the refractive index increases and fundamental band gap E_g^{opt} decreases from 2.58 to 2.21 eV as the tellurium concentration increases from 0 to 1. Furthermore, it was also found that the variation of optical band gap with composition shows quadratic behavior.*

Keywords: *$ZnSe_{1-x}Te_x$ thin film, nanocrystalline, Spectroscopic ellipsometry, bandgap.*

Introduction

Wide band gap semiconductors and their ternary alloys ($E_g^{opt} \approx$ 1 eV up to 3 eV) which are produced from the combination of groups II and VI have attracted intensive studies for many years due to their great potentials for a variety of applications, in particular in the field of optoelectronic devices, visible region light emitting devices, light detecting devices, photovoltaic conversion (solar cells), X-ray and _-ray detection [J.K. Furdyna (1988), Y.R. Lee et al (1988), U.V. Desnica (1998) , Y.D. Kim et al (1994), T. Holden et al (1997), S. Lee et al (1198), H.P. Wagner et al (1998), B. Sermage et al (1998), E. R. Shaaban et al (2008)]. Among many of the II–VI semiconductors compounds is the ternary alloy $ZnSe_{1-x}Te_x$ which is obtained from the combination of the ZnSe (Eg = 2.69 eV) and ZnTe (Eg = 2.25 eV) binary compounds. Previously, different spectroscopic techniques like hotoluminescence (PL) and photoconductivity (PC) were used to investigate the different optical transitions and the absorption process associated with these transitions in $ZnSe_{1-x}Te_x$ compound [M.J.S.P. Brasil et al (1991)]. Recently, the bulk sample of $ZnSe_xTe_{1-x}$ has been synthesized using conventional solid state reaction method, in which stoichiometric amount of the binary constituents of ZnSe and ZnTe powders were placed together and heated in a sealed silica tube at 1370 K for 24 h [M.M. El-Nahass et al (1996)]. Differen deposition techniques have also been used to synthesize the thin film of $ZnSe_{1-x}Te_x$. Such techniques include molecular beam epitaxy (MBE) of $ZnSe_xTe_{1-x}$ on GaAs [P.R. Newbury et al (1989)] and InP substrates [W. Lin, B.X. Yang et al(1999)] and physical vapor transport method [S.U. Ching-Hua et al (2000)].

© The authors. Published by Info Media Group & Anglisticum Journal, Tetovo, Macedonia.
Selection and peer-review under responsibility of ICNHBAS, 2013 http://www.nhbas2013.com

Since $ZnSe_{1-x}Te_x$ material is widely used as optical waveguide and cladding layers which intended to increase the optical confinement of the light waves [F.C. Peiris et al (1999), S.P. Guo, L. Zeng et al(2001), O. Maksimov et al (2001), A. Huynh et al (2003), D. Pereda Cubian et al(2003)]. In the present paper, the optical properties of different compositions of $ZnSe_{1-x}Te_x$ films are investigated in terms of spectroscopic ellipsometry by using three layer models. The photon energy used in this study covers the ranges below and above the band gap. Spectroscopic ellipsometry (SE) is a non-destructive and sensitive technique to measure the optical response of materials. By measuring the change in the polarization state, i.e., psi (ψ) and delta (Δ), of the light reflected off the surface of a film and subsequently utilizing an appropriate optical/dispersion model, one can extract precisely the optical properties and determine accurately the thickness of the film under study.

Experimental

Preparation of the bulk material

A series of polycrystalline bulk samples of $ZnSe_{1-x}Te_x$ ($0.1 \le x \le 1$) were prepared from mixing stoichiometric amounts of high purity (99.999% produced by Aldrich) analytical grade of ZnTe and ZnSe powders according to the following relation: $xZnTe + (1 - x)ZnSe \rightarrow ZnSe_{1-x}Te_x$.

At room temperature, the powders were mixed together in a mechanical ball mortar for about 30 min. After that, the mixed powders were then pressed into a circular disk shape pellet. Such pellets were used as the starting materials from which the thin film will be prepared

Preparation of thin films

Polycrystalline thin films samples of $ZnSe_{1-x}Te_x$ ($0 \le x \le 1$) were prepared by electron beam evaporation method using high vacuum coating unit type Edward 306Auto. The glass substrates used for deposition, of type corning No. 1022, were carefully cleaned using ultrasonic hot bath, distilled water and pure alcohol. Before the evaporation process started, the compressed disks of bulk $ZnSe_{1-x}Te_x$ ($0 \le x \le 1$) were loaded in a graphite boat and the vacuum system was left for a while to reach a pressure as low as 9×10^{-7} mbar. The conditions of evaporation were fully controlled by the rate of evaporation which was set at 2 nm/min and substrate temperature which was kept at room temperature. To ensure good homogenous of the film thickness, the substrates were rotated at low speed (2 rpm). During deposition process, the film thickness and the rate of evaporation were monitored using quartz crystal monitor attached to the vacuum system. Finally, the thicknesses of the deposited films were independently checked using F20 profile meter set up [M. Emam-Ismail et al (2010), E. R. Shaaban et al (2009), M. El-Hagary et al (2010)]. The structure of the prepared samples was examined by XRD analysis (Shimadzu X-ray diffractometry 6000, Japan with CuKα radiation with $\lambda = 0.15418$ nm). The intensity data were collected by step scan modes a 2θ range between 10 and 70 with step size 0.02^o and step time of 0.6 s. Pure silicon ≈ Si 99.9999 % was used as internal standard. The SE parameters (ψ and Δ) for $ZnSe_{1-x}Te_x$ films were measured with a rotating-compensator instrument (J.A. Woollam, M-2000) in the wavelength range 400–1100 nm. The data were acquired at angle of incidence of 70◦.

© The authors. Published by Info Media Group & Anglisticum Journal, Tetovo, Macedonia.
Selection and peer-review under responsibility of ICNHBAS, 2013 http://www.nhbas2013.com

All the measurements were conducted at room temperature. The optical constants of the $ZnSe_{1-x}Te_x$ films were determined by fitting the model function to the measured data using J.A. Woollam Corporation developed WVASE32 program.

Structural characterization

Fig.1 shows X-ray diffraction spectra of ZnSe, ZnTe powder and a simulate scan for both in terms of Rietveld refinement according to ZnSe and ZnTe cards using X'Pert HighSore (version 1.0e) program. Fig. 2 shows the room temperature XRD of the $ZnSe_{1-x}Te_x$ ($0 \leq x \leq 1$) films deposited on a glass substrate. The XRD patterns reveal that the as-deposited films were polycrystalline in nature. The analysis of the XRD of the as-deposited films of $ZnSe_{1-x}Te_x$ ($0 \leq x \leq 1$) indicates that the obtained films have cubic zinc-blend type structure (JCPDS 80-0021 and 75-2085). The XRD of the as deposited ZnSe film shows preferred orientation along (1 1 1) plane, note that the (2 2 2) peak is magnified (800 times) and is not plotted to same scale as peak (1 1 1) [C. Huang et al (2009)]. With further increasing of tellurium content into ZnSe matrix, the intensity of the two extra diffraction peaks (2 2 0) and (311) increases, indicating good crystallinity of the films. Finally, for ZnTe film three diffraction peaks are observed for planes (1 1 1), (2 2 0) and (3 1 1), respectively. These observations agree very well with the previous reported results for ZnSe, ZnTe and their mixed compounds [M.M. El-Nahass et al (1996), E. Bacaksiz et al (2009), T. Mahalingam et al (2012), J. Dutta et al (1994)]. The crystallites size (D_v) of $ZnSe_{1-x}Te_x$ ($0 \leq x \leq 1$) films was calculated by analyzing the XRD data using the Scherrer's formula, $D_v = k\lambda/\beta\cos(\theta)$; where β describes the structural broadening, which is the difference in integral X-ray peak profile width between the sample and a standard (silicon) and is given by $\beta=\sqrt{\beta_{obs}^2-\beta_{std}^2}$. It is observed that the crystallite size decrease till x = 50 % and increase with increasing Te content at expense of Se content in $ZnSe_{1-x}Te_x$ ($0 \leq x \leq 1$) as shown in Fig. 3.

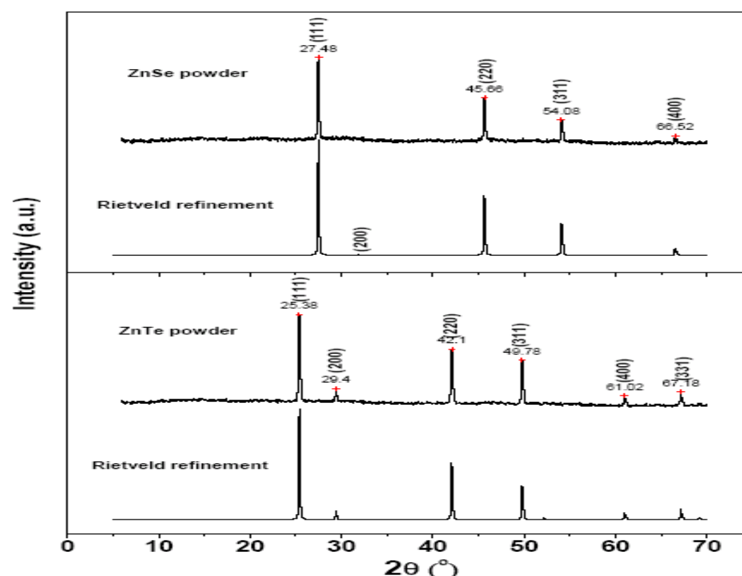

Fig.1: X-ray diffraction spectra of ZnSe, ZnTe powder and a simulate scan for both in terms of Rietveld refinement according to ZnSe and ZnTe cards using X'Pert HighSore (version 1.0e) program.

© The authors. Published by Info Media Group & Anglisticum Journal, Tetovo, Macedonia.
Selection and peer-review under responsibility of ICNHBAS, 2013 http://www.nhbas2013.com

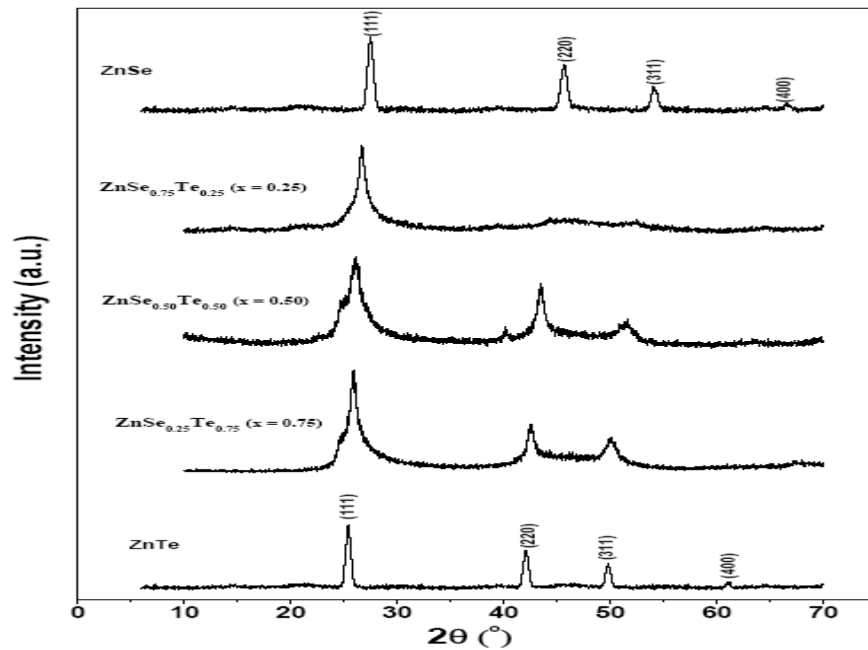

Fig. 2: The XRD patterns of different composition of ZnSe $_{(1-x)}$Te$_x$ thin films onto glass substrates

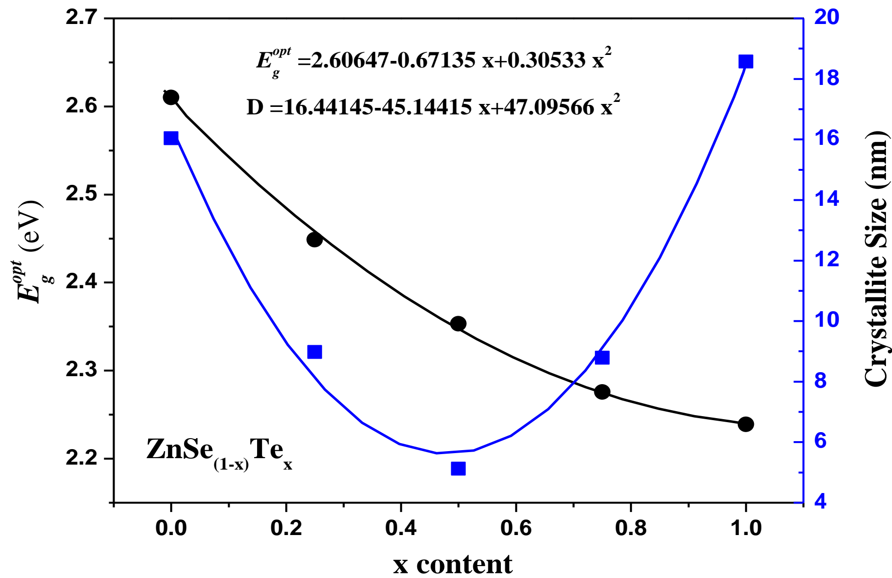

Fig. 3. Variation of crystallites size calculated from the plane (1 1 1) and optical band gap with the fraction x for the as-deposited polycrystalline ZnSe$_{1-x}$Te$_x$ thin films.

© The authors. Published by Info Media Group & Anglisticum Journal, Tetovo, Macedonia.
Selection and peer-review under responsibility of ICNHBAS, 2013 http://www.nhbas2013.com

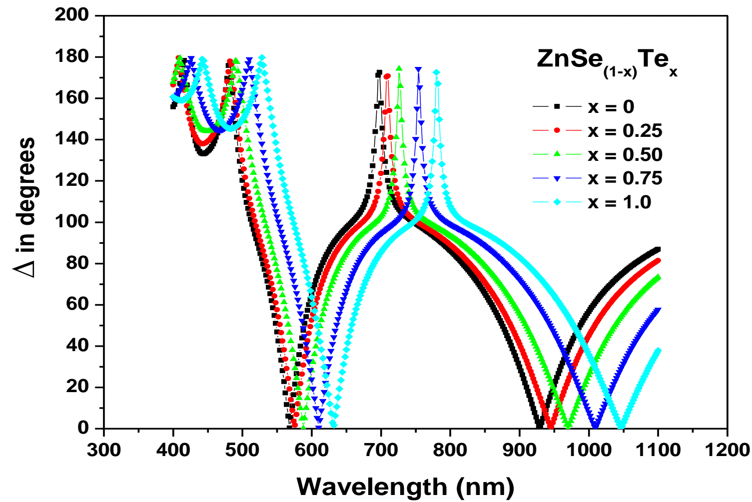

Fig. 4: Spectral ellipsometric data ψ and Δ for nanocryatalline $ZnSe_{(1-x)}Te$

Optical properties

Calculation of optical constants in terms of spectroscopic ellipsometry data

The optical properties of $ZnSe_{1-x}Te_x$ ($0 \leq x \leq 1$) thin films have been primarily studied by spectroscopic ellipsometry (SE), which measures the relative changes in amplitude and phase of the linearly polarized monochromatic incident light upon oblique reflection from the film surface. It is worth mentioned that the optical properties of $ZnSe_{1-x}Te_x$ thin films measured by SE as a function of Te composition x have not been reported to date. The appropriate experimental setups are required which determine non-redundant optical parameters from a general anisotropic sample. Generalized Ellipsometry (GE) comprises theory and experiment of anisotropy in layered samples. The experimental parameters obtained by standard SE (ψ and Δ) are related to the microstructure and optical properties as defined by [H. Fujiwara et al (2007)]: $\rho = \frac{r_p}{r_s} = \tan\psi \exp(i\,\Delta)$ (1)

Here r_s and r_p are the complex Fresnel's reflection coefficients of the light polarized parallel (r_p) and perpendicular (r_s) to the plane of incidence, respectively. The layer model analysis, based on Fresnel's coefficients of reflection, was performed on the measured ellipsometric angles. The spectral dependencies of ψ and Δ for $ZnSe_{1-x}Te_x$ films are shown in Fig. 4. The spectral dependencies of ψ and Δ were fitted in appropriate model to extract the film thickness and optical constants, i.e. refractive index (n) and extinction coefficient (k), using a least square regression analysis and a weighted root mean square error function. The optical constants of $ZnSe_{1-x}Te_x$ are accurately described with a three layer models: upper layer (rough layer)/ absorbing $ZnSe_{1-x}Te_x$ layer/ glass substrate. The upper layer corresponds to the microscopic roughness obtained by SE is well correlated with the mean square error.

© The authors. Published by Info Media Group & Anglisticum Journal, Tetovo, Macedonia.
Selection and peer-review under responsibility of ICNHBAS, 2013 http://www.nhbas2013.com

The program is based on the least square regression to obtain the unknown fitting parameters and their maximum confidence limit. The procedure is to vary fitting parameters to minimize the difference between the measured and calculated ψ and Δ values. The Levenberg–Marquardt regression algorithm was used for minimizing the mean-squared error (MSE) [H. Fujiwara (2007)]:

$$MSE=\frac{1}{2N\text{-}M}\sum_{i=1}^{N}\left(\left(\frac{\psi_i^{mod}-\psi_i^{exp}}{\sigma_{\psi,i}^{exp}}\right)^2+\left(\frac{\Delta_i^{mod}-\Delta_i^{exp}}{\sigma_{\Delta,i}^{exp}}\right)^2\right) \quad (2)$$

which has been used to judge the quality of the fit between the measured and the modeled data and is minimized in the fit. Here N is the number of measured ψ and Δ pairs included in the fit, M is the number of fit parameters and i is the summation index. Also, ψ_i^{exp} , Δ_i^{exp} and ψ_i^{mod}, Δ_i^{mod} are the experimental and modeled values of ψ and Δ, respectively. $\sigma_{\psi,i}^{exp}$ and $\sigma_{\Delta,i}^{exp}$ are the experimental standard deviations in ψ and Δ respectively, which were calculated from the known error bars on the calibration parameters and the fluctuation of the measured data over averaged cycle of the rotating polarizer and analyzer. Eq. (2) has the *2N* and *M* in perfactor because there are two measured values included in the calculation for each ψ and Δ pair. The calculated data ψ_i^{th} and Δ_i^{th} are generated by using the appropriate models as shown in Fig. 5 (a,b) with corresponding dispersion relations [J.W. Park et al (2008)]. The spectral dependencies of ψ and Δ determined for $ZnSe_{1-x}Te_x$ films on glass substrate are depicted in Fig. 5(a-e) for x= 0-100% and x = 0.1, the spectra show Fabry-Perot interference oscillations over the entire wavelength range originating from the multiple reflections within the films [Y. Yamada et al (2008)]. Clearly, there is a good agreement between the measured data (symbols) and the model fit (line) in the entirely measured wavelength range. We note that the shapes of the curves with their particular interference peaks are correctly reproduced but small differences between experimental and calculated parameters could be observed. The estimated thicknesses for the surface roughness layer and for the $ZnSe_{1-x}Te_x$ dense layer are shown in the inset of the Figs. 5 (a-e). The fitted optical constants, i.e. the refractive indices and extinction coefficients of different thicknesses of $ZnSe_{1-x}Te_x$ films are presented in Fig. 6 and Fig. 7, respectively. As can be seen the refractive index increases gradually with increasing of the Te content in the $ZnSe_{1-x}Te_x$ at any wavelength. The increase in refractive index with increasing Te content may be attributed to the increase in the polarizability. The atomic radii of Se and Te are 1.42 Å, and 1.4 Å, respectively [S. Tolansky et al (1970)]. The larger atomic radius of the atom, the larger will be its polarizability. Therefore, such dependence of the refractive index on the Te content of the investigated films can be explained on the basis of Lorentz-Lorenz equation in which a direct proportion between the polarizability and refractive index is established [S. R. Elliott (2000)]. Thus, substituting of more polarizable Te atoms by less polarisable Ze may lead to an increase of refractive index. Fig. 7 shows the dispersion of the extinction coefficient $k(\lambda)$ of $ZnSe_{1-x}Te_x$ thin films. As shown in this figure the extinction coefficient increases with increasing Te content.

© The authors. Published by Info Media Group & Anglisticum Journal, Tetovo, Macedonia.
Selection and peer-review under responsibility of ICNHBAS, 2013 http://www.nhbas2013.com

Optical energy band gap analysis

The optical absorption coefficient, α as shown in Fig 8 of crystalline $ZnSe_{1-x}Te_x$ films with different composition $0 \leq x \leq 1$ is evaluated from the obtained k values from the relation: $\alpha = \frac{4\pi k}{\lambda}$ (3)

The optical energy band gap, E_g^{opt}, of the $ZnSe_{1-x}Te_x$ ($0 \leq x \leq 1$) films can be determined from optical measurements in semiconductors by fitting the data to the Tauc's relation [J. Tauc(1974)]:

$(\alpha h\nu)^{1/\delta} = \alpha_0 (h\nu - E_g^{opt})$ (4)

where α_0 is a constant and δ is an exponent that depends on the type of the band transitions involved; e.g. $\delta = 1/2$ *or* $3/2$ for allowed direct interband transitions and forbidden direct interband transitions, respectively. Fig. 9 shows the variation of $(\alpha h\nu)^2$ with the photon energy, $h\nu$, for $ZnSe_{1-x}Te_x$ films. From the obtained results, a direct electronic transition across the band gap of the films is observed. The extrapolation of the linear part of the curves to the photon energy axis would give the optical band gap that varied in the range, 2.58 to 2.21 eV with the increase of Te concentration from 0 to 1. The variation of band gap of polycrystalline $ZnSe_{1-x}Te_x$ films with Te composition was found to increase parabolic (shown in Fig. 3). The red shift of the fundamental optical energy gap with increasing Te content is attributed to the continuous replacement of the Se atoms by Te. This reduction of the optical energy gap can be explained on the basis of the bond energy within zincblende crystal structure (ZnSe, ZnTe). The crystal structure of polycrystalline ZnSe is mainly zincblende structure in which the zinc atom is chemically bonded to four Se atoms in the form of tetrahedral structure where Zn Se bond has energy value of order 170.7 ± 25.9 kJ mol−1. As the Te concentration increases more Te atoms will replace Se atoms within zincblende structure. This simply means the concentration of the Zn Te bonds will increases on the expanses of Zn Se bonds. The Zn Te bonds have lower bond energy (117.6 ± 18.0 kJ mol−1) than Zn Se bonds (170.7 ± 25.9 kJ mol−1). Consequently, the lower bond energy of Zn Te bonds leads to a reduction of the optical band gap of the ternary alloys $ZnSe_{1-x}Te_x$ with increasing Te concentration [G. De Maria et al (1965), M. Grade et al (1982)].

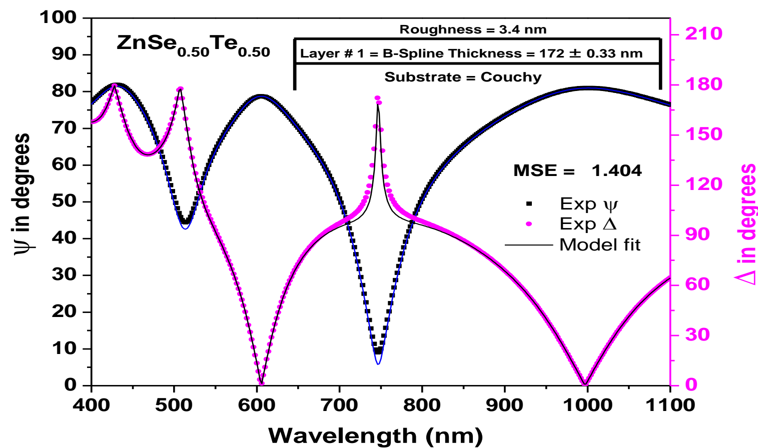

© The authors. Published by Info Media Group & Anglisticum Journal, Tetovo, Macedonia.
Selection and peer-review under responsibility of ICNHBAS, 2013 http://www.nhbas2013.com

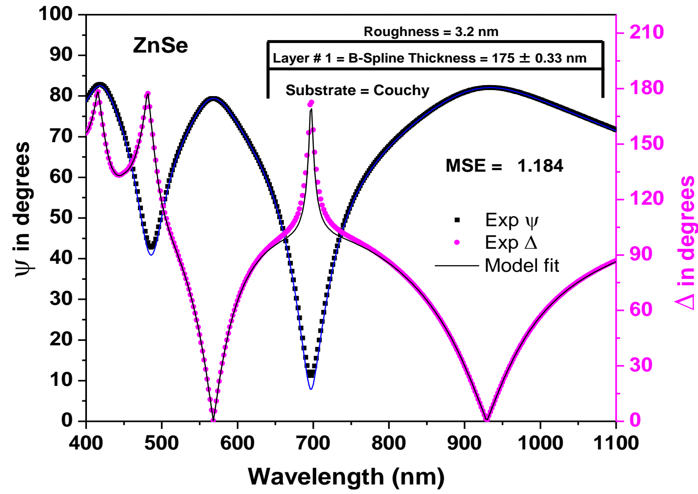

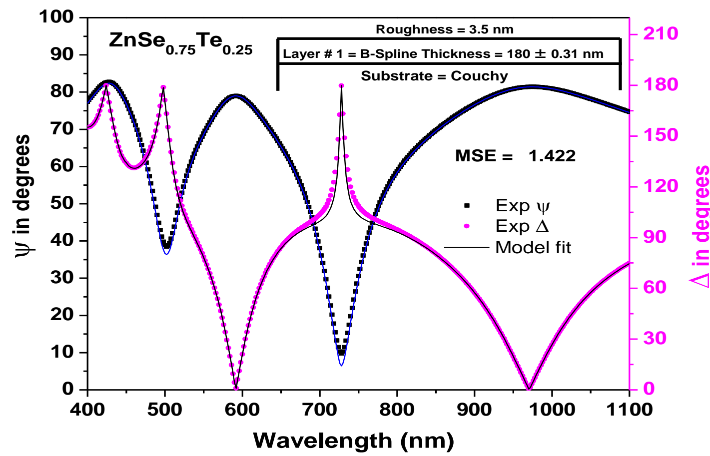

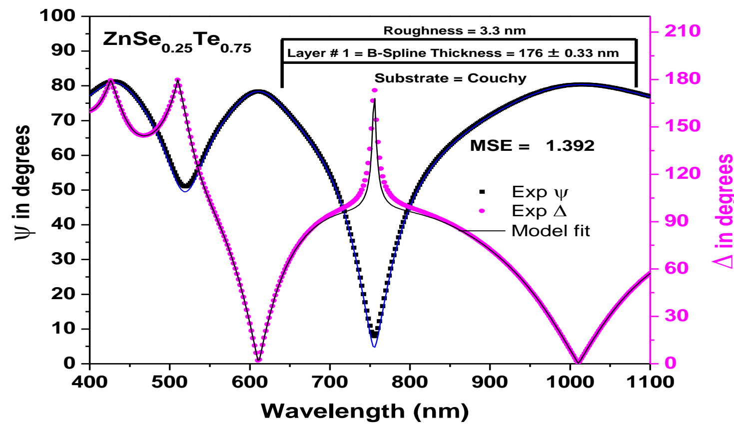

© The authors. Published by Info Media Group & Anglisticum Journal, Tetovo, Macedonia.
Selection and peer-review under responsibility of ICNHBAS, 2013 http://www.nhbas2013.com

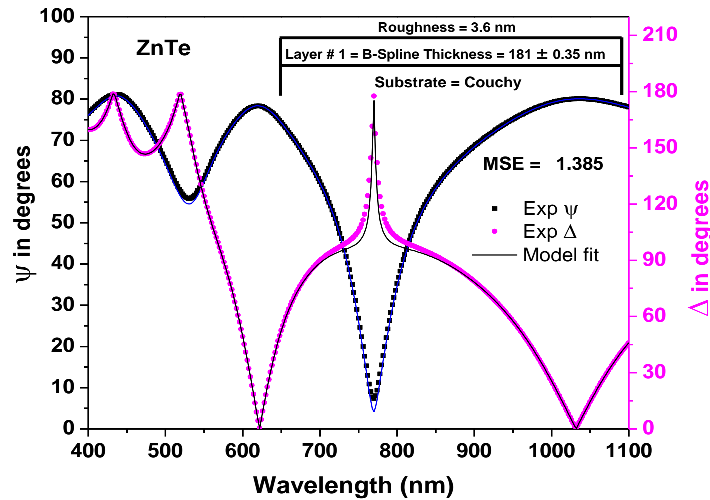

Fig. 5: Spectral ellipsometric data (ψ and Δ) for nanocryatalline $ZnSe_{(1-x)}Te_x$ films grown on glass substrate. Experimental results are indicated by symbols and the solid lines represent model fit data.

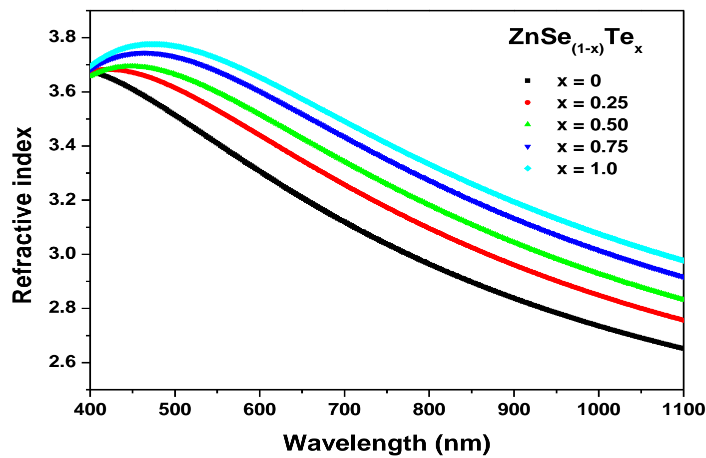

Fig. 6: The spectral dependence of refractive index *n* for nanocryatalline $ZnSe_{(1-x)}Te_x$ films with different compositions (x = 0, 0.25, 0.50, 0.75 and 1.0).

© The authors. Published by Info Media Group & Anglisticum Journal, Tetovo, Macedonia.
Selection and peer-review under responsibility of ICNHBAS, 2013 http://www.nhbas2013.com

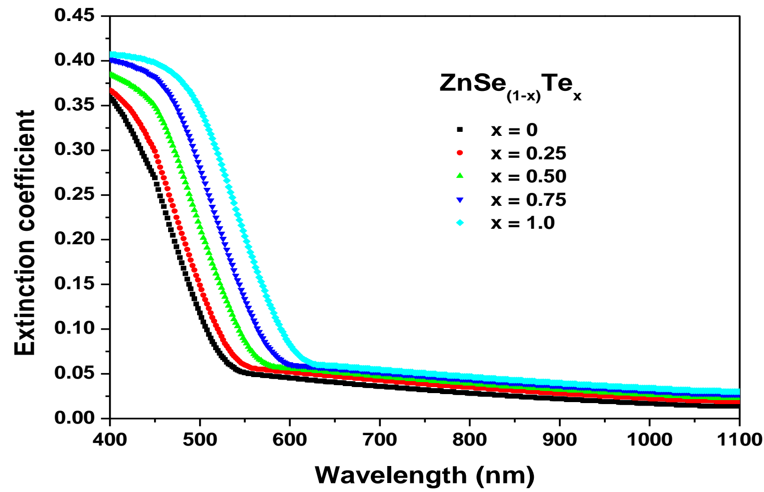

Fig. 7: The dispersion of extinction coefficient *(k)* for nanocryatalline $ZnSe_{(1-x)}Te_x$ films with different compositions (x = 0, 0.25, 0.50, 0.75 and 1.0).

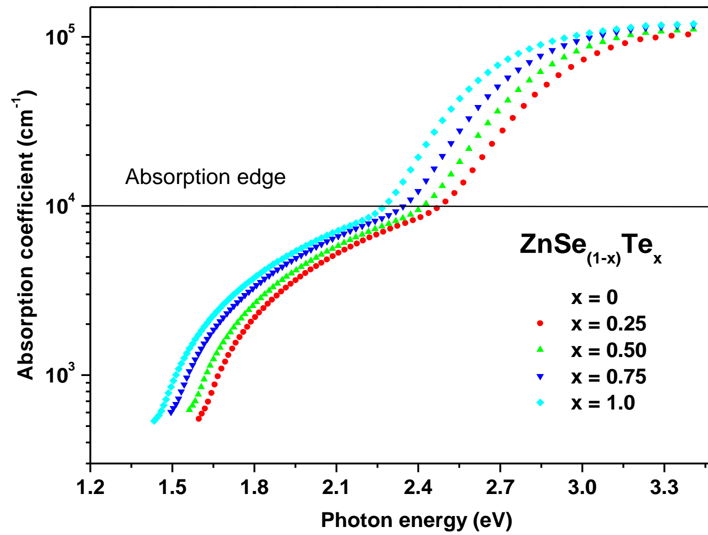

Fig. 8: Plot of absorption coefficient, α with the photon energy, $h\nu$, for as-deposited $ZnSe_{(1-x)}Te_x$ films with different compositions (x = 0, 0.25, 0.50, 0.75 and 1.0) films

© The authors. Published by Info Media Group & Anglisticum Journal, Tetovo, Macedonia.
Selection and peer-review under responsibility of ICNHBAS, 2013 http://www.nhbas2013.com

Conclusions

Nanocrystalline $ZnSe_{1-x}Te_x$ thin films were deposited on glass substrate by electron beam deposition method. XRD characterization reveals that all the deposited films have polycrystalline zinc blend structure. The optical properties of the $ZnSe_{1-x}Te_x$ nanocrystalline films were determined by spectroscopic ellipsometric measurements in a range of 400–1100 nm at room temperature. The optical characterization shows that the refractive index of the polycrystalline $ZnSe_{1-x}Te_x$ increases gradually with increasing of the Te content at any wavelength. The increase in refractive index with increasing Te content may be attributed to the increase in the polarizability, where the atomic radii of Se and Te are 1.42 Å, and 1.4 Å, respectively. The fundamental band gap decreases from 2.58 to 2.21 eV with increasing tellurium content. The red shift of the fundamental optical energy gap with increasing Te content is attributed to the continuous replacement of the Se atoms by Te. This reduction of the optical energy gap can be explained on the basis of the bond energy within zincblende crystal structure (ZnSe, ZnTe). Te concentration increases more Te atoms will replace Se atoms within zincblende structure. This simply means the concentration of the Zn Te bonds will increases on the expanses of Zn Se bonds. The Zn Te bonds have lower bond energy (117.6 ± 18.0 kJ mol−1) than Zn Se bonds (170.7 ± 25.9 kJ mol−1). Consequently, the lower bond energy of Zn Te bonds leads to a reduction of the optical band gap of the ternary alloys $ZnSe_{1-x}Te_x$ with increasing Te concentration.

References

1. J.K. Furdyna, Journal of Applied Physics 64 (1988) R29.
2. Y.R. Lee, A.K. Ramadas, L.A. Kolodziejski, R.L. Gunshor, Physical Review B 38 (1988) 13143.
3. U.V. Desnica, Progress in Crystal Growth and Characterization of Materials 36 (1998) 291.
4. Y.D. Kim, M.V. Klein, S.E. Ren, Y.C. Chang, Physical Review B 49 (1994) 7262.
5. T. Holden, P. Ram, F.H. Pollak, Physical Review B 56 (1997) 4037.
6. S. Lee, F. Michl, U. Rossler, M. Dobrowolska, J.K. Furdyna, Physical Review B 57 (1998) 9695
7. H.P. Wagner, M. Kuhnelt, W. Langbein, J.M. Hvam, Physical Review B 58 (1998) 10494.
8. B. Sermage, S. Petiot, C. Tanguy, Si. Dang Le, R. Andre, Journal of Applied Physics 83 (1998) 7903.
9. E. R. Shaaban, M. F. Kaid, E. Moustafa and A. Adel, J. Physics. D: Applied Physics. 41 (2008) 53125301.
10. M.J.S.P. Brasil, R.E. Nahory, F.S. Turco-Sandroff, H.L. Gilchrist, R.J. Martin, Applied Physics Letters 58 (1991) 2509.
11. M.M. El-Nahass, B.A. Khalifa, A.M. Abd El-Rahman, R. El-Ariny, Applied Physics A 63 (1996) 81.
12. P.R. Newbury, K. Shahzad, J. Petruzzello, D.A. Cammack, Journal of Applied Physics 66 (1989) 4950.
13. W. Lin, B.X. Yang, S.P. Guo, A. Elmoumni, F. Fernandez, M.C. Tamargo, Applied Physics Letters 78 (1999) 2608.
14. S.U. Ching-Hua, S. Feth Shen Zhu, S.L. Lehoczky, Journal of Applied Physics 88 (2000) 5148.
15. F.C. Peiris, S. Lee, U. Bindley, J.K. Furdyna, Journal of Applied Physics 86 (1999)719.
16. S.P. Guo, L. Zeng, M.C. Tamargo, Applied Physics Letters 78 (2001) 1.
17. O. Maksimov, S.P. Guo, L.Z. Eng, M.C. Tamargo, F.C. Peiris, J.K. Furdyno, Journal

© The authors. Published by Info Media Group & Anglisticum Journal, Tetovo, Macedonia.
Selection and peer-review under responsibility of ICNHBAS, 2013 http://www.nhbas2013.com

ISSN 1857-8179 (paper). ISSN 1857-8187 (online). http://www.anglisticum.mk
Proceedings of the 1st International Conference on New Horizons in Basic and Applied Science, Hurghada – Egypt, Vol 1(1), 2013.

of Applied Physics 89 (2001) 2202.
18. A. Huynh, J. Tignon, G. Keller, Ph. Roussignol, R. Andre, R. Romestain, L.S. Dang, Physical Review B 68 (2003) 165340.
19. D. Pereda Cubian, M. Haddad, R. Andre, R. Frey, G. Roosen, J. Arce, C. Diego, L. Flytzains, Physical Review B 67 (2003) 45308.
20. M. Emam-Ismail, E.R. Shaaban, M. El-Hagary, I. Shaltout, Philosophical Magazine 90 (2010) 3499.
21. E. R. Shaaban, I Kansal, S. H. Mohamed, J M. F. Ferreira, Physica B: Condensed matter 404 (2009) 3571.
22. M. El-Hagary, M. Emam-Ismail, S.H. Mohamed, A. Hamid, S.S. Althoyaib, ThinSolid Films 518 (2010) 4058.
23. C. Huang, H. Weng, Y. Jiang, H. Ueng, Vacuum 83 (2009) 313.
24. E. Bacaksiz, S. Aksu, N. Ozer, M. Tomakin, A. Ozcelik, Applied Surface Science 256 (2009) 1566.
25. T. Mahalingam, V. Dhanasekaran, R. Chandramohan, J.K. Rhee, Journal of Materials Science 47 (2012) 1950.
26. J. Dutta, R. Pal, S. Chaudhuri, A.K. Pal, Journal of Physics D: Applied Physics 27 (1994) 1538.
H. Fujiwara, in:Spectroscopic Ellipsometry: Principles and Applications, Wiley, West Sussex, UK, 2007.
27. J.W. Park, K.N. Choi, S.H. Baek , K.S. Chung, H. Lee, J. Korean Phys. Soc. 52 (2008) 1868.
28. Y. Yamada, K. Tajima, M. Okada, S. Bao, M. Tazawa, K. Yoshimura, A. Roos, Phys. Stat. Sol. C (2008)1105.
29. S. Tolansky, Multiple-Beam Interference Microscopy of Metals, vol. 55, Academic Press, London, 1970.
30. S. R. Elliott, The physics and chemistry of solids, Wiley, Chichester, 2000.
31. J. Tauc, Amorphous and Liquid Semiconductor, New York Plenum, 1974.
32. G. De Maria, P. Goldfinger, P.L. Malaspina, V. Piacente, Transactions of the Faraday Society 61 (1965) 2146.
33. M. Grade, W. Hirschwald, B. Bunsenges, Physical Chemistry 86 (1982) 899.

© The authors. Published by Info Media Group & Anglisticum Journal, Tetovo, Macedonia.
Selection and peer-review under responsibility of ICNHBAS, 2013 http://www.nhbas2013.com